Electron capture and loss by kilo-electron-volt oxygen atoms in collisions with He, H_2, N_2, and O_2

B. G. Lindsay, W. S. Yu, K. F. McDonald,* and R. F. Stebbings
Department of Physics and Astronomy, and Rice Quantum Institute, Rice University, 6100 Main Street, Houston, Texas 77005-1892, USA
(Received 25 May 2004; published 5 October 2004)

Absolute differential cross sections are reported for electron capture and loss by (1–5)-keV oxygen atoms incident on He, H_2, N_2, and O_2 for scattering angles between 0.02° and 1.73° in the laboratory frame. The form of the differential cross sections is seen to vary significantly with energy and between different targets. Differences between the present O-atom electron-loss cross sections and those for H atoms reported previously imply that the underlying physical mechanism may not be the same. The integral cross sections, also reported here, are consistent with most previous studies. The consensus of the available electron-loss data suggests that the cross sections of Fogel *et al.* [Soviet Phys. JETP **35**, 601 (1959)] are in error.

DOI: 10.1103/PhysRevA.70.042701 PACS number(s): 34.70.+e, 34.50.Lf

I. INTRODUCTION

The importance of charge-changing processes in keV atomic collisions is well established, and these reactions have been studied very extensively both experimentally and theoretically. The bulk of the prior work has, however, focused on the simplest processes and the most accessible collision systems, while more technically formidable reactions, such as those considered here, have received scant attention. The only previously reported measurements of O-atom capture and loss cross sections at energies below 1 MeV known to us are the total cross section measurements of Fogel *et al.* [1], Jorgensen *et al.* [2], Olsen and Hvelplund [3], and Brackmann and Fite [4], which together encompass the energy range 20 keV to 500 keV. There appear to be no prior studies for energies below 20 keV or that include angular differential cross section data. In this work, absolute differential cross sections (DCSs) for electron capture and loss by (1–5)-keV O atoms incident on He, H_2, N_2, and O_2 for scattering angles between 0.02° and 1.73° in the laboratory frame are presented, together with the corresponding integral cross sections.

While some of the processes chosen for study here are relevant to controlled fusion edge plasmas [5] and particle precipitation into the Jovian atmosphere [6], the main area of application of the present measurements is modeling of energetic particle precipitation into the earth's upper atmosphere. Significant fluxes of energetic oxygen ions and neutral atoms have been observed during geomagnetic storms [7], and the effect of these particle fluxes on the atmosphere is dependent on the magnitude of the various cross sections for collision with atmospheric neutral species and on the angular distribution of the scattered particles [8]. Cross sections for charge transfer of O^+ ions are already available [2,9–14] and, together with the present measurements, represent a comprehensive set of oxygen charge-changing data for use by atmospheric modelers.

II. APPARATUS AND EXPERIMENTAL METHOD

The apparatus shown in Fig. 1 and the experimental method have both been described in detail previously [15]. CO is admitted to a magnetically confined plasma ion source. Ions are extracted from the source through a small aperture, accelerated, and focused to form a beam of the desired energy. Two confocal 60-sector magnets are used to select ions of the desired mass-to-charge ratio. The O^+ ions then enter a charge-transfer cell (CTC) where some of them are converted to fast neutral O atoms via charge transfer with CO_2. An electric field ($\sim$300 V/cm) applied via deflection plates DP1 removes residual ions from the beam, and the O atoms pass through a pair of laser-drilled apertures to form a beam with an angular divergence of approximately 0.006°. The collimated O beam passes through a short target cell and impacts a position-sensitive detector (PSD1) located 68 cm beyond the target cell. A set of deflection plates (DP2) is utilized to deflect fast product ions emerging from the target cell through an angle of approximately 5° onto a second position-sensitive detector (PSD2).

In order to measure the differential electron-capture or -loss cross section, a target gas is admitted to the target cell and the angles of scatter of the O^- or O^+ ions, formed through electron capture or loss by the primary O atoms, are determined from their positions of impact on PSD2. The O-atom flux incident on the target is determined by combining the number of O atoms that impact PSD1 with the number of oxygen ions produced. These measurements, together with the target number density, the target length, and the relative detection efficiency of the two PSDs, are sufficient to determine the absolute differential and integral cross sections.

Measurement of the target number density and target length is straightforward but evaluation of the PSD's relative detection efficiency requires that a number of factors be considered [16,17]. It has been shown previously that the detec-

*Present address: School of Applied and Engineering Physics, College of Engineering, Cornell University, Clark Hall, Ithaca, NY 14853–2501, USA.

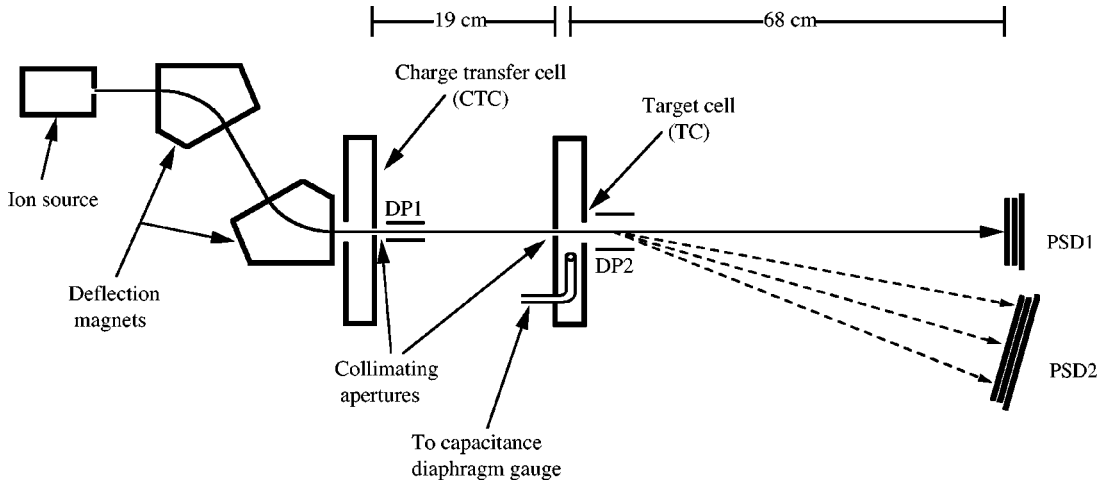

FIG. 1. Schematic of the apparatus.

tion efficiency of this type of PSD is essentially identical for ions and atoms at these energies [18], is invariant over a very wide range of ion masses [17], and is primarily determined by the open-area ratio of the first microchannel plate when the device is appropriately biased [17]. In this instance, relative calibration of the two PSDs, for both ions and atoms, is therefore accomplished by alternately deflecting an O^+-ion beam onto PSD1 and PSD2. In practice, the detection efficiencies are quite similar: PSD2's efficiency is 6–12 % lower than that for PSD1, depending upon the energy of the incident ions.

As indicated in the Introduction, the scattering processes studied here present formidable experimental difficulties. Perhaps chief among these is the potential influence of any excited O atoms that may be present in the projectile beam on the measurements. The effect of internal energy on O-atom electron-capture and -loss cross sections does not appear to have been studied previously, but it is well known that metastable oxygen ions often have significantly different electron-transfer cross sections from ground-state oxygen ions [10], and it is reasonable to suppose that the capture and loss cross sections studied here may depend upon the internal energy of the O atoms.

As the O-atom beam is produced via charge transfer of an O^+ beam, the electronic state of the O atoms is influenced by the electronic state of the O^+ precursor ions, the charge-transfer gas used, and the ions' kinetic energy. The energy defects for the reaction channels through which the atoms are produced are also extremely important, as it has been shown repeatedly that charge transfer is most likely to occur via reaction channels with small energy defects, and that channels with significant energy defects are often suppressed quite dramatically [10–12]; this effect is energy dependent and decreases as the kinetic energy increases. It is also worth noting that the influence of these various factors has only been established qualitatively, e.g., by Lindsay and Latimer [19]. Here, CO_2 is utilized as the charge-transfer gas because reaction of either $O^+(^4S)$ ground-state or $O^+(^2D,^2P)$ metastable ions, which are produced by the ion source in comparable numbers [11,20], is likely to result in the formation of $O(^3P)$ ground-state atoms due to the availability of near-

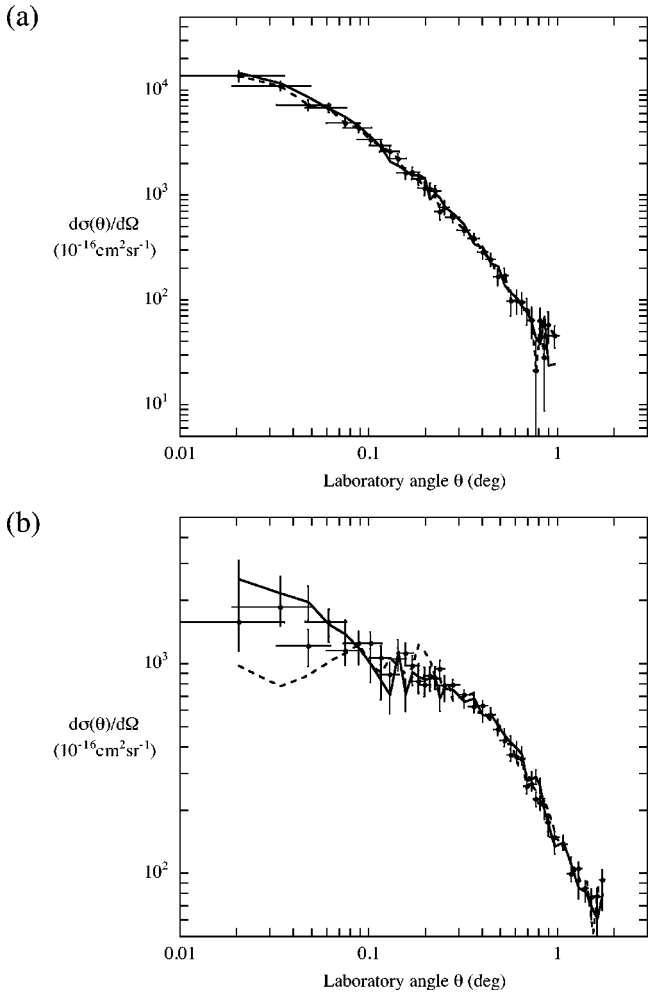

FIG. 2. Comparison of the differential cross sections for (a) electron capture and (b) electron loss by 3-keV O atoms in collisions with N_2 using CO_2, N_2, and Kr charge-transfer gases. With CO_2 (●); N_2 (—); Kr (- - -).

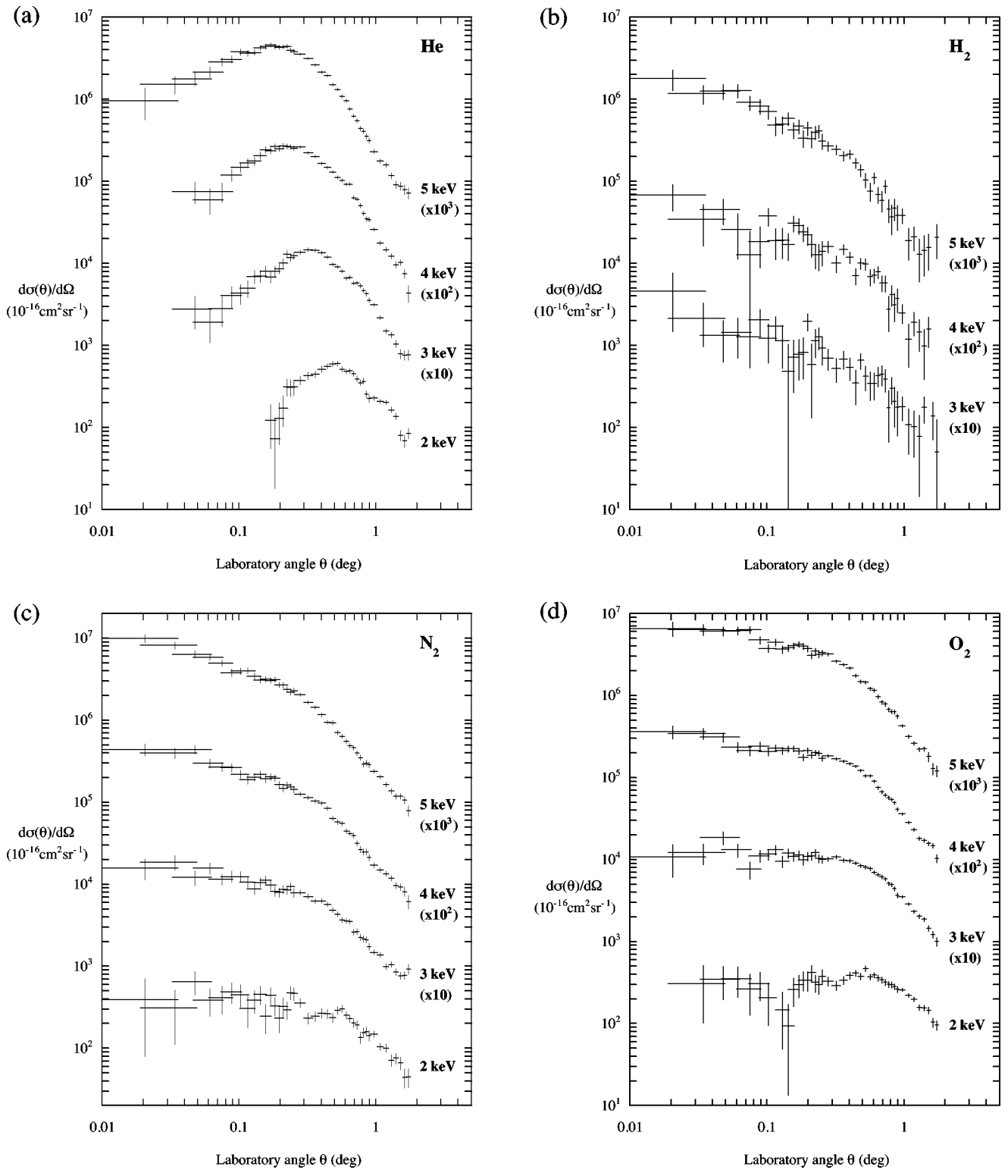

FIG. 3. Absolute differential cross sections for electron loss by O atoms in collisions with (a) He, (b) H_2, (c) N_2, and (d) O_2. For convenience of presentation the data have been multiplied by the factors indicated.

resonant reaction channels with small energy defects [10,21]. Undoubtedly, some $O(^1D)$ and $O(^1S)$ metastable atoms will also be produced, but because the energy defects involved are greater than for formation of $O(^3P)$ atoms they will be formed in smaller numbers.

Based on the above qualitative argument, it is reasonable to expect that the use of CO_2 will result in an O beam consisting primarily of $O(^3P)$ atoms, but the possibility that the results may be affected by residual metastables is by no means precluded. Therefore, to check for the influence of

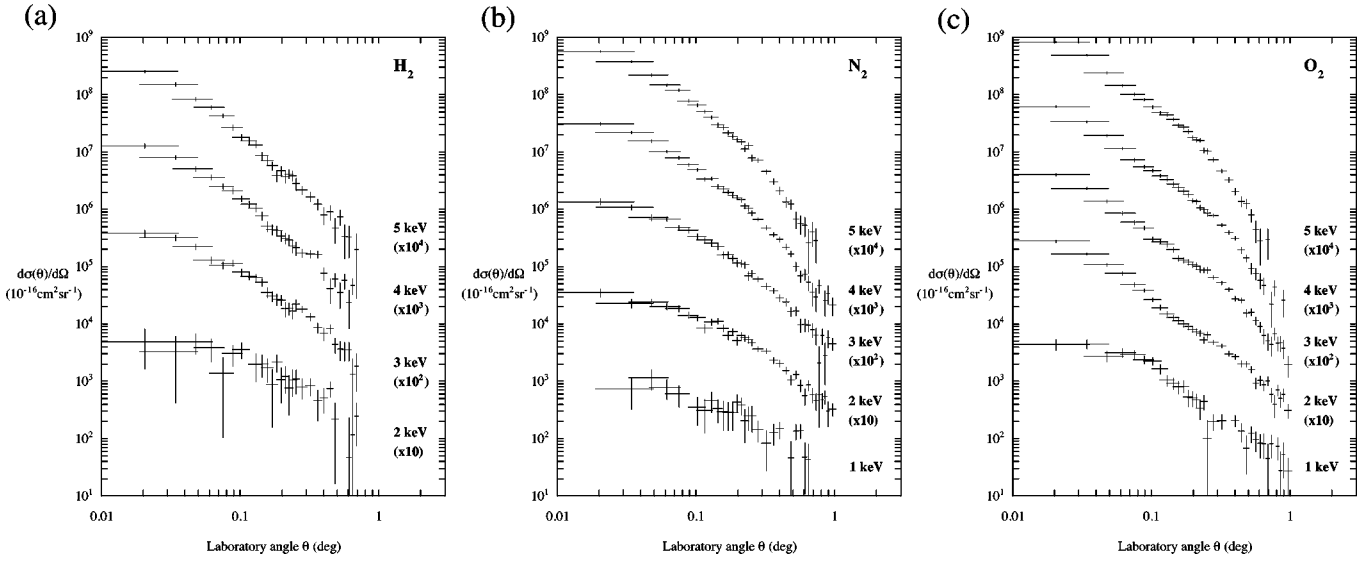

FIG. 4. Absolute differential cross sections for electron capture by O atoms in collisions with (a) H_2, (b) N_2, and (c) O_2. For convenience of presentation the data have been multiplied by the factors indicated.

TABLE I. Laboratory frame differential O-He electron-loss cross sections, where E is the projectile energy and the numbers in square brackets represent powers of ten.

Laboratory angle θ (deg)	$d\sigma(\theta)/d\Omega$ (10^{-16} cm^2 sr^{-1})			
	$E=2$ keV	$E=3$ keV	$E=4$ keV	$E=5$ keV
0.020±0.015				9.67±4.00[2]
0.048±0.015		2.79±1.19[2]	7.52±2.17[2]	1.79±0.32[3]
0.075±0.015		2.82±1.11[2]	7.56±1.96[2]	2.88±0.32[3]
0.157±0.015		8.10±1.16[2]	2.44±0.20[3]	4.41±0.27[3]
0.280±0.025	3.74±0.44[2]	1.37±0.07[3]	2.63±0.09[3]	3.56±0.11[3]
0.525±0.025	6.04±0.38[2]	9.17±0.40[2]	1.12±0.04[3]	1.33±0.05[3]
0.968±0.056	2.29±0.13[2]	3.14±0.12[2]	2.61±0.11[2]	2.32±0.12[2]
1.732±0.056	8.54±1.22[1]	7.72±1.02[1]	4.35±1.00[1]	7.22±1.06[1]

TABLE II. Laboratory frame differential O-H_2 electron-loss cross sections, where E is the projectile energy and the numbers in square brackets represent powers of ten.

Laboratory angle θ (deg)	$d\sigma(\theta)/d\Omega$ (10^{-16} cm^2 sr^{-1})		
	$E=3$ keV	$E=4$ keV	$E=5$ keV
0.020±0.015	4.59±3.10[2]	6.83±2.42[2]	1.80±0.51[3]
0.048±0.015	1.34±0.71[2]	4.57±1.59[2]	1.27±0.27[3]
0.075±0.015	1.28±0.74[2]	1.28±1.22[2]	9.18±1.80[2]
0.157±0.015	7.28±4.60[1]	3.12±0.68[2]	4.27±0.92[2]
0.280±0.025	7.05±2.06[1]	1.62±0.26[2]	2.70±0.38[2]
0.525±0.025	4.25±1.41[1]	9.91±1.60[1]	1.05±0.21[2]
0.968±0.056	1.81±0.59[1]	2.52±0.67[1]	3.88±0.81[1]
1.732±0.056			2.09±0.93[1]

TABLE III. Laboratory frame differential O-N_2 electron-loss cross sections, where E is the projectile energy and the numbers in square brackets represent powers of ten.

Laboratory angle θ (deg)	$d\sigma(\theta)/d\Omega$ (10^{-16} cm^2 sr^{-1})			
	$E=2$ keV	$E=3$ keV	$E=4$ keV	$E=5$ keV
0.020±0.015	3.95±3.15[2]	1.58±0.43[3]	4.40±0.73[3]	9.93±1.15[3]
0.048±0.015	6.51±2.01[2]	1.21±0.25[3]	4.39±0.50[3]	6.39±0.61[3]
0.075±0.015	4.16±1.53[2]	1.15±0.18[3]	2.71±0.32[3]	5.01±0.42[3]
0.157±0.015	2.46±0.95[2]	1.13±0.13[3]	1.93±0.18[3]	3.17±0.24[3]
0.280±0.025	3.59±0.44[2]	7.93±0.48[2]	1.26±0.07[3]	2.07±0.08[3]
0.525±0.025	2.90±0.30[2]	4.31±0.28[2]	5.75±0.33[2]	7.15±0.39[2]
0.968±0.056	1.50±0.12[2]	1.48±0.09[2]	1.71±0.10[2]	2.40±0.12[2]
1.732±0.056	4.47±1.16[1]	9.30±1.15[1]	6.14±1.09[1]	7.91±1.13[1]

TABLE IV. Laboratory frame differential O-O_2 electron-loss cross sections, where E is the projectile energy and the numbers in square brackets represent powers of ten.

Laboratory angle θ (deg)	$d\sigma(\theta)/d\Omega$ (10^{-16} cm^2 sr^{-1})			
	$E=2$ keV	$E=3$ keV	$E=4$ keV	$E=5$ keV
0.020±0.015		1.08±0.47[3]	3.63±0.67[3]	6.58±1.31[3]
0.048±0.015	3.48±1.52[2]	1.87±0.35[3]	3.12±0.44[3]	6.16±0.82[3]
0.075±0.015	2.67±1.39[2]	7.65±1.85[2]	2.14±0.29[3]	6.37±0.68[3]
0.157±0.015	2.63±1.01[2]	1.10±0.15[3]	2.27±0.20[3]	4.06±0.37[3]
0.280±0.025	3.30±0.44[2]	1.02±0.06[3]	1.85±0.08[3]	3.22±0.14[3]
0.525±0.025	4.71±0.36[2]	8.15±0.41[2]	1.05±0.05[3]	1.46±0.07[3]
0.968±0.056	2.60±0.14[2]	3.56±0.14[2]	3.63±0.13[2]	4.30±0.19[2]
1.732±0.056	9.63±1.34[1]	1.00±0.12[2]	1.04±0.12[2]	1.22±0.18[2]

TABLE V. Laboratory frame differential O-H_2 electron-capture cross sections, where E is the projectile energy and the numbers in square brackets represent powers of ten.

Laboratory angle θ (deg)	$d\sigma(\theta)/d\Omega$ (10^{-16} cm^2 sr^{-1})			
	$E=2$ keV	$E=3$ keV	$E=4$ keV	$E=5$ keV
0.020±0.015	4.95±3.30[2]	3.82±0.54[3]	1.29±0.12[4]	2.56±0.18[4]
0.048±0.015	4.95±1.91[2]	2.24±0.27[3]	5.15±0.51[3]	8.43±0.68[3]
0.075±0.015	1.40±1.30[2]	1.07±0.16[3]	2.55±0.30[3]	4.32±0.40[3]
0.157±0.015	1.72±0.75[2]	3.56±0.68[2]	5.12±1.01[2]	7.10±1.21[2]
0.280±0.025	7.95±3.04[1]	1.82±0.23[2]	1.75±0.29[2]	2.21±0.36[2]
0.525±0.025		3.68±1.36[1]	3.59±1.72[1]	7.51±2.30[1]
0.968±0.056	1.13±0.88[1]	1.22±0.55[1]	1.66±0.75[1]	1.51±0.92[1]

TABLE VI. Laboratory frame differential O-N_2 electron-capture cross sections, where E is the projectile energy and the numbers in square brackets represent powers of ten.

Laboratory angle θ (deg)	$d\sigma(\theta)/d\Omega$ (10^{-16} cm^2 sr^{-1})				
	$E=1$ keV	$E=2$ keV	$E=3$ keV	$E=4$ keV	$E=5$ keV
0.020±0.015		3.55±0.59[3]	1.37±0.17[4]	3.11±0.19[4]	5.70±0.27[4]
0.048±0.015	1.16±0.45[3]	2.43±0.31[3]	7.23±0.80[3]	1.58±0.09[4]	2.23±0.11[4]
0.075±0.015	6.10±2.53[2]	1.88±0.25[3]	4.86±0.52[3]	7.99±0.49[3]	1.22±0.07[4]
0.157±0.015	3.00±1.60[2]	8.50±1.14[2]	1.62±0.22[3]	2.28±0.19[3]	2.69±0.21[3]
0.280±0.025	1.48±0.59[2]	3.66±0.37[2]	6.13±0.64[2]	6.76±0.46[2]	7.20±0.53[2]
0.525±0.025	1.38±0.42[2]	1.33±0.21[2]	1.71±0.30[2]	1.02±0.19[2]	6.86±2.27[1]
0.968±0.056		3.33±0.84[1]	4.57±1.09[1]	2.13±0.74[1]	

TABLE VII. Laboratory frame differential O-O_2 electron-capture cross sections, where E is the projectile energy and the numbers in square brackets represent powers of ten.

Laboratory angle θ (deg)	$d\sigma(\theta)/d\Omega$ (10^{-16} cm^2 sr^{-1})				
	$E=1$ keV	$E=2$ keV	$E=3$ keV	$E=4$ keV	$E=5$ keV
0.020±0.015	4.46±1.06[3]	2.81±0.16[4]	4.10±0.23[4]	6.21±0.27[4]	8.27±0.30[4]
0.048±0.015	2.78±0.59[3]	1.08±0.07[4]	1.40±0.09[4]	1.95±0.10[4]	2.43±0.11[4]
0.075±0.015	2.99±0.47[3]	4.90±0.37[3]	6.00±0.45[3]	7.35±0.49[3]	1.03±0.06[4]
0.157±0.015	8.08±2.02[2]	1.14±0.13[3]	1.41±0.16[3]	2.40±0.20[3]	2.93±0.22[3]
0.280±0.025	2.01±0.60[2]	4.85±0.41[2]	6.60±0.51[2]	7.85±0.50[2]	7.46±0.52[2]
0.525±0.025	1.24±0.40[2]	1.62±0.22[2]	1.62±0.22[2]	9.47±1.98[1]	8.07±2.17[1]
0.968±0.056	2.77±1.82[1]	3.13±0.83[1]	1.95±0.75[1]		

TABLE VIII. Absolute integral electron-loss and electron-capture cross sections for O on He, H_2, N_2, and O_2. The angular range for the integral cross sections is $0°-1.79°$.

Energy (keV)	Electron loss (10^{-16} cm^2)				Electron capture (10^{-16} cm^2)		
	He	H_2	N_2	O_2	H_2	N_2	O_2
1	0.182±0.026		0.137±0.020	0.173±0.024		0.113±0.019	0.174±0.025
2	0.629±0.068	0.0235±0.0073	0.355±0.039	0.627±0.068	0.0423±0.0078	0.162±0.019	0.256±0.028
3	0.900±0.092	0.0576±0.0073	0.550±0.057	0.993±0.102	0.0839±0.0095	0.288±0.031	0.288±0.030
4	1.08±0.11	0.0930±0.0108	0.732±0.074	1.21±0.12	0.107±0.012	0.316±0.033	0.330±0.034
5	1.29±0.13	0.148±0.016	0.992±0.100	1.57±0.16	0.152±0.017	0.338±0.035	0.394±0.040

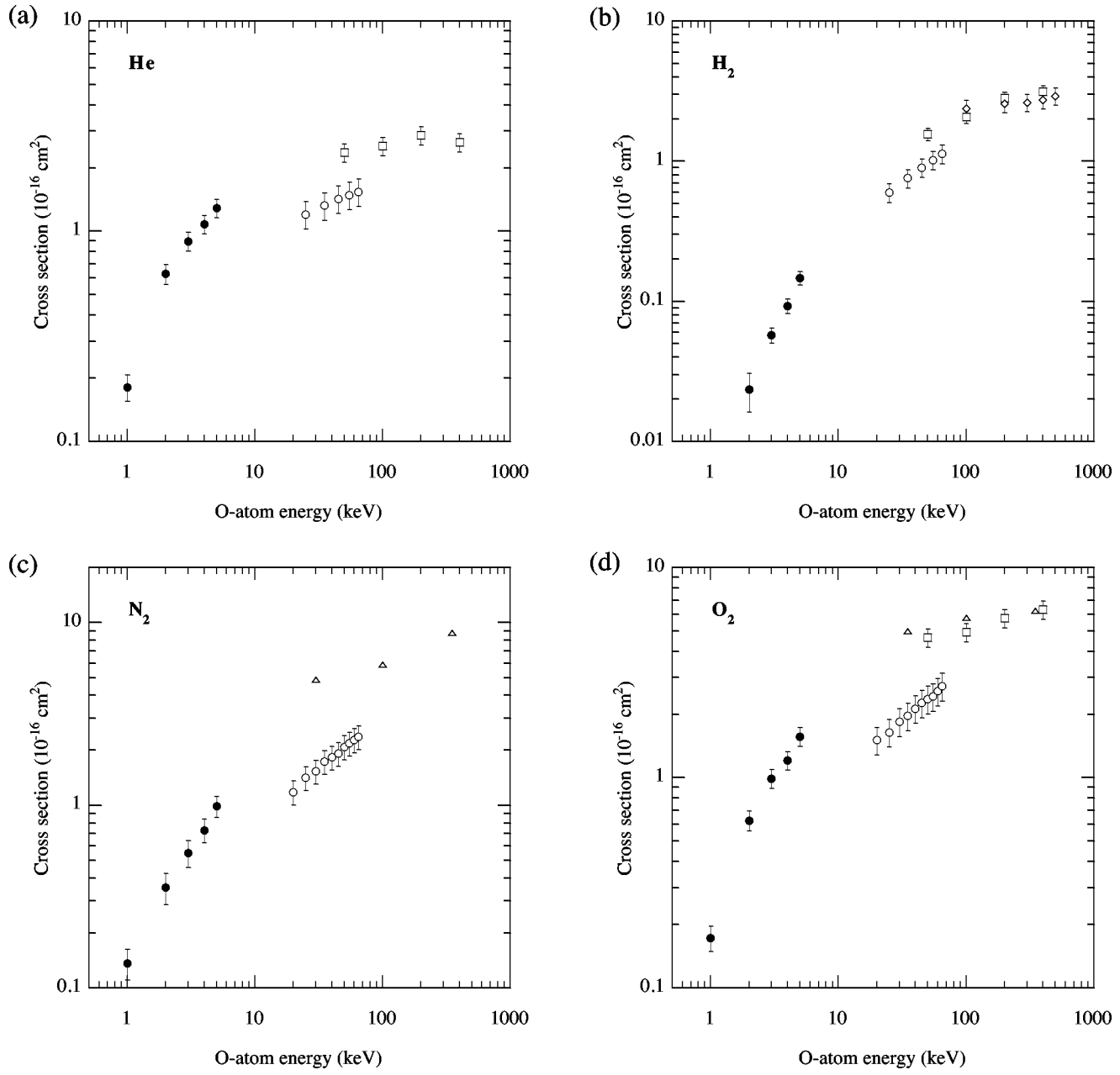

FIG. 5. Integral cross sections for electron loss by O atoms in collisions with (a) He, (b) H_2, (c) N_2, and (d) O_2 compared to previous total cross section measurements. Present results (●); Fogel *et al.* [1] (○); Jorgensen *et al.* [2] (□); Olsen and Hvelplund [3] (◇); Brackmann and Fite [4] (△).

metastables, tests were carried out using two other charge-transfer gases, N_2 and Kr. As for CO_2, collisions of O^+ with N_2 seem likely to result in production of $O(^3P)$ products [10,11], but, due to the position of the energy levels in Kr, it is probable that collisions of $O^+(^2D)$ and $O^+(^2P)$ metastable ions with Kr will result in formation of a significant number of $O(^1D)$ and $O(^1S)$ excited atoms. The DCSs for electron capture and loss obtained using the three charge-transfer gases are shown in Fig. 2. Clearly, the data obtained using CO_2 and N_2 agree very well, providing strong evidence that both gases result in production of $O(^3P)$ atoms and that the effect of any residual metastables is small. For Kr, the electron-capture results are in excellent agreement with the others, and the agreement for the electron-loss process is also quite good, except at very small angles. Based upon the data in Fig. 2, a persuasive argument may be made that the use of CO_2 as a charge-transfer gas results in a primarily ground-state O beam, and that the influence of metastable O atoms on the reported data is not significant.

Another experimental difficulty arises from the fact that the measured cross sections are generally quite small compared to those for reneutralization of the charged products. It is therefore necessary to adjust conditions in the target cell so that the probability is low that a charged product ion is reneutralized after it is formed. To this end, the pressure in the 1.4-mm-long target cell is maintained at approximately

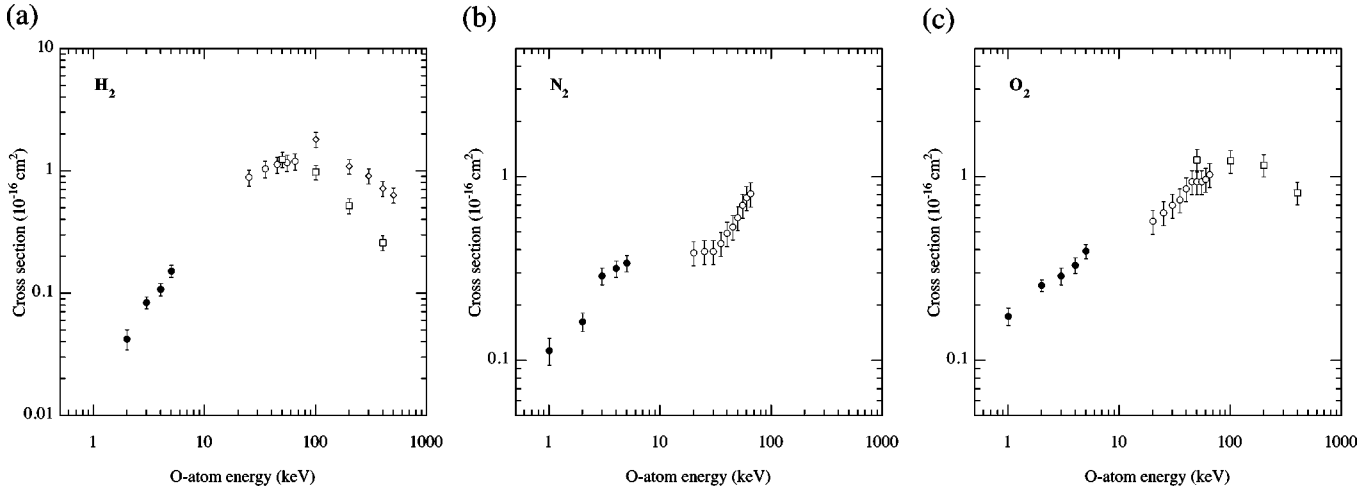

FIG. 6. Integral cross sections for electron capture by O atoms in collisions with (a) H_2, (b) N_2, and (c) O_2 compared to previous total cross section measurements. Present results (●); Fogel *et al.* [1] (○); Jorgensen *et al.* [2] (□); Olsen and Hvelplund [3] (◇); Brackmann and Fite [4] (△).

35 mtorr, which allows for reasonable count rates while keeping secondary collisions to an acceptable level. This arrangement is necessarily a compromise, and corrections of as much as 8% are made to the electron-loss cross sections, utilizing published cross section data [11–13], to account for the loss of O^+ ions via charge transfer. Such corrections cannot be made for the electron-capture cross sections because information on electron loss by O^- ions is virtually nonexistent. The high-energy measurements of Jorgensen *et al.* [2] suggest that the magnitude of the correction needed for the electron-capture cross sections is also on the order of 8%. Note that no correction is needed for He because the O^+ -He charge-transfer cross section is very small [14].

Because of the finite angular range subtended by the detector in this type of experiment, it is not possible to collect all of the fast ionic products. The extent to which the integral cross section approximates the total cross section may, however, be estimated from the rapidity with which the DCS decreases with increasing scattering angle. This suggests that the integral He and H_2 electron loss cross sections and the electron capture cross sections, particularly at the higher projectile energies, are a reasonable approximation to the total cross sections. The slower decrease with angle of the N_2 and O_2 electron loss DCSs suggests that the corresponding integral cross sections should be viewed merely as lower limits to the total cross sections.

III. RESULTS AND DISCUSSION

The measured differential electron-capture and -loss cross sections are shown in Fig. 3 and Fig. 4, and selected values are tabulated in Tables I–VII. In addition to the statistical uncertainties shown on the graphs, there are additional systematic uncertainties that are generally ±10–15 % (Table VIII). The angular uncertainties arise from the finite primary beam size and the angular resolution used for analysis. From Fig. 3, it can be seen that there is considerable variation in the shapes of the electron-loss DCSs. The He data contrast sharply with the more typical forward-peaked DCSs for the other targets, and it appears that glancing, large-impact-parameter O-He collisions are unlikely to result in production of O^+. There is some suggestion of structure in the DCSs but, given the statistical scatter in the data, it is difficult to say how significant it may be. The electron-capture cross sections, which are shown in Fig. 4, are plainly more forward peaked than those for electron loss and show no discernible structure. To our knowledge, no other experimental data exist with which the present results may be compared and theoretical approaches are not yet well enough developed to handle these types of collision problems. The few calculations that are available are for H rather than O, and even these do not agree satisfactorily with experiment in this energy range [22].

It is perhaps worth comparing this study with the earlier H-atom study by Smith *et al.* [15], which considered scattering by He, Ar, H_2, N_2, and O_2. In that work, it was found that all of the H-atom electron-loss cross sections were forward peaked, including that for He. Also, in contrast to the N_2 and O_2 O-atom DCSs, which vary little with angle at 2 keV, Smith *et al.* [15] found the analogous H-N_2, and H-O_2 DCSs to fall off just as rapidly at 2 keV as at 5 keV. In a pair of related studies by Van Zyl *et al.* [23] it was asserted that the functional forms of the electron-loss and direct-scattering DCSs are similar, except at small angles. This conclusion is, by and large, supported by the Smith *et al.* [15] data for the targets that they studied also. However, if the present electron-loss data are compared to the O-atom direct-scattering measurements of Smith *et al.* [24], the dissimilarity is quite obvious; the present low-energy DCSs are very much flatter than the direct-scattering measurements. The very significant differences between electron loss by O and by H would seem to indicate underlying differences in the reaction mechanisms. Interestingly, the H-capture data of Smith *et al.* [15] are similar to the present O-atom measurements, suggesting that these processes may be amenable to explanation in terms of the same basic model.

The present integral cross sections and their associated uncertainties are tabulated in Table VIII. The uncertainties

are primarily due to the PSD relative efficiency calibration, the uncertainty in the ratio of ion to atom detection efficiencies, and the repeatability of the measurements. The integral data are compared to the high-energy measurements of Fogel *et al.* [1], Jorgensen *et al.* [2], Olsen and Hvelplund [3], and Brackmann and Fite [4] in Figs. 5 and 6. Although the present data do not overlap in energy with any of the other work, it is readily apparent that the present electron-loss and electron-capture cross sections are consistent with those of the other workers, with the exception of the electron-loss data of Fogel *et al.* [1]. The consensus formed by the present data and those of Jorgensen *et al.* [2], Olsen and Hvelplund [3], and Brackmann and Fite [4] clearly favors higher electron-loss cross sections than reported by Fogel *et al.* [1], indicating that the latter are probably in error.

IV. CONCLUSION

Absolute differential cross sections are reported for electron capture and loss by (1–5)-keV oxygen atoms incident on He, H_2, N_2, and O_2 for scattering angles between 0.02° and 1.73° in the laboratory frame. The form of the DCSs is seen to vary significantly with energy and between different targets. Differences between the present O-atom electron-loss DCSs and those for H atoms reported by Smith *et al.* [15] imply that the underlying physical mechanism may not be the same. The integral cross sections, also reported here, are consistent with most previous high-energy studies. The consensus of the available electron-loss data suggests that the cross sections of Fogel *et al.* [1] are in error.

While the present work very significantly advances our knowledge of these processes, it also emphasizes the lack of experimental data and the undeveloped state of theory.

ACKNOWLEDGMENTS

We gratefully acknowledge support by the National Science Foundation under Grants No. 0108734 and No. 0139202, and by the Robert A. Welch Foundation.

[1] Ia. M. Fogel, V. A. Ankudinov, and D. V. Pilipenko, Sov. Phys. JETP **35**, 601 (1959).
[2] T. Jorgensen, C. E. Kuyatt, W. W. Lang, D. C. Lorents, and C. A. Sautter, Phys. Rev. **140**, A1481 (1965).
[3] J. O. Olsen and P. Hvelplund, J. Phys. B **7**, 1331 (1974).
[4] R. T. Brackmann and W. L. Fite, Air Force Weapons Laboratory Report No. AFWL-TR-68-96 (unpublished). The Brackmann and Fite data shown in this paper were taken from a review by R. C. Dehmel, H. K. Chau, and H. H. Fleischmann, At. Data **5**, 231 (1973).
[5] R. K. Janev, H. P. Winter, and W. Fritsch, in *Atomic and Molecular Processes in Fusion Edge Plasmas*, edited by R. K. Janev (Plenum Press, New York, 1995).
[6] M. Horanyi, T. E. Cravens, and J. H. Waite, J. Geophys. Res., [Space Phys.] **93**, 7251 (1988); T. E. Cravens and G. M. Eisenhower, Icarus **100**, 260 (1992).
[7] E. G. Shelley, R. G. Johnson, and R. D. Sharp, J. Geophys. Res. **77**, 6104 (1972); R. D. Sharp, R. G. Johnson, and E. G. Shelley, *ibid.* **81**, 3283 (1976); *ibid.* **81**, 3292 (1976).
[8] M. Ishimoto, G. J. Romick, and C.-I. Meng, J. Geophys. Res., [Space Phys.] **97**, 8619 (1992); M. Ishimoto, M. R. Torr, P. G. Richards, and D. G. Torr, *ibid.* **91**, 5793 (1986); D. V. Bisikalo, V. I. Shematovich, and J.-C. Gérard, *ibid.* **100**, 3715 (1995).
[9] R. F. Stebbings, A. C. H. Smith, and H. Ehrhardt, J. Geophys. Res. **69**, 2349 (1964); J. A. Rutherford and D. A. Vroom, J. Chem. Phys. **61**, 2514 (1974); A. D. Irvine and C. J. Latimer, J. Phys. B **24**, L145 (1991); X. Li, Y.-L. Huang, G. D. Flesch, and C. Y. Ng, J. Chem. Phys. **106**, 1373 (1997); B. G. Lindsay, D. R. Sieglaff, K. A. Smith, and R. F. Stebbings, J. Geophys. Res., [Space Phys.] **106**, 8197 (2001); T. Kusakabe, H. Nakanishi, A. Iida, K. Hosomi, H. Tawara, M. Sasao, and Y. Nakai, J. Phys. B **34**, 4809 (2001). A very large number of papers have been published on this topic and only a representative few are referenced here.
[10] T. F. Moran and J. B. Wilcox, J. Chem. Phys. **69**, 1397 (1978).
[11] B. G. Lindsay, R. L. Merrill, H. C. Straub, K. A. Smith, and R. F. Stebbings, Phys. Rev. A **57**, 331 (1998).
[12] D. R. Sieglaff, B. G. Lindsay, K. A. Smith, and R. F. Stebbings, Phys. Rev. A **59**, 3538 (1999).
[13] D. R. Sieglaff, B. G. Lindsay, R. L. Merrill, K. A. Smith, and R. F. Stebbings, J. Geophys. Res., [Space Phys.] **105**, 10631 (2000).
[14] B. G. Lindsay and R. F. Stebbings, Phys. Rev. A **67**, 022715 (2003).
[15] G. J. Smith, L. K. Johnson, R. S. Gao, K. A. Smith, and R. F. Stebbings, Phys. Rev. A **44**, 5647 (1991).
[16] R. S. Gao, P. S. Gibner, J. H. Newman, K. A. Smith, and R. F. Stebbings, Rev. Sci. Instrum. **55**, 1756 (1984).
[17] H. C. Straub, M. A. Mangan, B. G. Lindsay, K. A. Smith, and R. F. Stebbings, Rev. Sci. Instrum. **70**, 4238 (1999).
[18] R. S. Gao, L. K. Johnson, D. A. Schafer, J. H. Newman, K. A. Smith, and R. F. Stebbings, Phys. Rev. A **38**, 2789 (1988); L. K. Johnson, R. S. Gao, C. L. Hakes, K. A. Smith, and R. F. Stebbings, *ibid.* **40**, 4920 (1989); R. S. Gao, L. K. Johnson, G. J. Smith, C. L. Hakes, K. A. Smith, N. F. Lane, R. F. Stebbings, and M. Kimura, *ibid.* **44**, 5599 (1991).
[19] B. G. Lindsay and C. J. Latimer, J. Phys. B **21**, 1617 (1988).
[20] Removal of the metastable O^+ ions using a filter cell, as described by Lindsay *et al.* (Ref. [11]), would have been advantageous in obtaining a ground-state O beam but would have resulted in an unacceptably low signal rate.
[21] B. G. Lindsay, D. R. Sieglaff, K. A. Smith, and R. F. Stebbings, J. Phys. B **32**, 4697 (1999).
[22] H. Levy II, Phys. Rev. **185**, 7 (1969); D. R. Bates, and A. Williams, Proc. Phys. Soc., London, Sect. A **70**, 306 (1957).
[23] B. Van Zyl, T. Q. Le, H. Neumann, and R. C. Amme, Phys. Rev. A **15**, 1871 (1977); H. Neumann, T. Q. Le, and B. Van Zyl, *ibid.* **15**, 1887 (1977).
[24] G. J. Smith, R. S. Gao, B. G. Lindsay, K. A. Smith, and R. F. Stebbings, Phys. Rev. A **53**, 1581 (1996).